Surface chemistry of mercury on zinc and copper

ARTICLE *in* METALLURGICAL AND MATERIALS TRANSACTIONS B · JANUARY 2006

Impact Factor: 1.46 · DOI: 10.1007/BF02735028

4 AUTHORS, INCLUDING:

Seshadri Seetharaman
KTH Royal Institute of Technology
402 PUBLICATIONS **2,516** CITATIONS
SEE PROFILE

Mats Göthelid
KTH Royal Institute of Technology
154 PUBLICATIONS **1,748** CITATIONS
SEE PROFILE

Surface Chemistry of Mercury on Zinc and Copper

D. ROSEBOROUGH, M. GÖTHELID, P. PALMGREN, and S. SEETHARAMAN

Thermal desorption Auger electron spectroscopy (TDAES) was used to investigate mercury adsorption on the surfaces of zinc (Zn) and copper (Cu) in the temperature interval of 85 to 298 K. The effects of chlorine and oxygen modifications on the surfaces have also been investigated within the same temperature interval. On single crystalline Zn(0001), no mercury was adsorbed under any temperature or deposition conditions. On polycrystalline Zn at 85 K, a monolayer (ML) of mercury adsorbed, whereas no measurable quantity was observed at room temperature (RT). Predeposited chlorine was removed by exposure to mercury, most probably through formation of volatile $HgCl_2$. Chlorine enhanced the adsorption of mercury on polycrystalline Cu at 87 K, whereas preoxidation reduced the coverage. Low temperatures (LTs) were conducive to mercury adsorption as compared to 298 K for the Cu systems studied. The physisorption of mercury on chlorine and oxygen layers at LTs is discussed, as well as the factors affecting the mechanism of adsorption at RTs. The desorption energies and surface enthalpies have been calculated for each system with mercury adsorption.

I. INTRODUCTION

MERCURY is a toxic element, damaging not only to humans, but also to the environment. As a result, international regulations are now being implemented to phase out its use in products and processes.[1] Dealing with mercury emissions from industrial sources has also become an important problem. Emissions levels are now being monitored more closely and, in some cases, companies have been forced to reduce their mercury emission levels.[2]

For steel plants fed by scrap metal, *viz.* electric arc furnace (EAF) steel plants, mercury emissions are particularly hard to control and predict. Because mercury can be found in devices such as electric switches in cars and batteries, scrap metal must be extremely well sorted to remove the sources before the metal is melted down. It is also believed that mercury may adsorb on the surface of zinc (Zn) present on the surface of the galvanized automobile plates in the scrap and copper (Cu) stored at subzero temperatures, thereby entering the production line with the raw material.[3] As the scrap is fed into the EAF, mercury is flashed off in the furnace because of its high vapor pressure compared to other metals. These discharges are partially collected in the emissions-control systems. Previous investigations have been made to correlate mercury emissions with a specific raw material, but have shown that this correlation is difficult to accomplish.[3]

Specific raw materials, such as dolomite, are known to contribute to mercury emissions in EAF steelmaking.[4] Gas and coal are finding increased use in the production of stainless steel, and it has been shown that even these raw materials contain small amounts of mercury.[5] However, the trace amounts of mercury that these materials contribute are not believed to account for the elevated levels of mercury found in residues, slag, and exhaust fumes. Currently, it is not well understood how mercury enters the EAF and which forms are the most significant.

With the rise of galvanized steel products since the 1980s,[6] more and more Zn has been entering the EAF with the steel scrap. Over the same time interval, mercury emissions have been noted to be increasing.[7] This may, in part, be due to more diligent mercury emissions measurements, but it is also based on a real increase in mercury emissions. The relationship between increased galvanized metals in the scrap and the increase in mercury emissions has, as yet, not been firmly established.

The motivation for studying mercury adsorption at different temperatures and surface conditions, therefore, stems from the need to determine the source of the mercury emissions, be it atmospheric deposition, precontamination due to alloying elements or raw materials, or galvanized scrap. Copper and Zn were chosen as obvious substrates. Copper and Zn are both relevant metals in EAF steelmaking, and Cu may enter the EAF with scrap containing electrical equipment. Zinc is of critical interest to steelmakers because of the increased use of galvanized scrap, and Zn also forms stable phases with mercury at low temperatures (LTs).[8] Iron has been studied previously with this respect[9] and found to adsorb mercury on clean but not oxidized surfaces.

Oxygen and chlorine were selected as coadsorbates with mercury. Oxygen naturally coats surfaces and chlorine is known to be reactive with mercury in the atmosphere.[10,11] The substrates are studied at LTs to determine desorption energies, specific desorption temperatures, and saturation coverages using thermal desorption Auger electron spectroscopy (TDAES). A comparative study is made at room temperature (RT). This verifies the temperature dependence of mercury adsorption and aims to investigate the factors affecting the mechanism of mercury adsorption. The present article aims also to discuss the effects of chlorine and oxygen modifications on the adsorption mechanism and mercury bonding on the surface of Cu and Zn.

II. PREVIOUS WORK

In 1989, Dowben *et al.*[12] studied the electronic structure of mercury overlayers on Cu(100). They suggest that mercury

D. ROSEBOROUGH, Doctoral Student, and S. SEETHARAMAN, Professor, are with the Department of Materials Science and Engineering, Royal Institute of Technology, 10044 Stockholm, Sweden. Contact e-mail: dianar@mse.kth.sc M. GÖTHELID, Associate Professor, and P. PALMGREN, Doctoral Student, are with the Materials and Semiconductor Physics Department, Royal Institute of Technology, 16440 Kista, Sweden.

Manuscript submitted November 23, 2005.

atoms are located 36.2 nm apart forming a $c(2 \times 2)$ structure on Cu(100) according to the phase diagram shown in Figure 1. This would presumably correspond to 0.5 monolayer (ML) of adsorbed mercury, where one ML is defined as the number of atoms on the ideal bulk terminated surface, either on the substrate or the overlayer ($\sim 1 \cdot 10^{15}$ atoms per cm^2).[13] At doses higher than 19 Langmuir (L) at temperatures below 230 K, mercury layers are disordered.

Dowben *et al.*[12] also calculated an isosteric heat of adsorption to 70 ± 4 kJ/mol for mercury on Cu(100) and suggested that there are strong attractive lateral interactions between the mercury atoms in the adlayer. In 1990, Li *et al.*[14] studied mercury and lead growth on Cu(001) at 150 K. It was found that mercury is too large to fit in the Cu lattice and that mercury overlayers ''buckle'' because of the mismatching of the lattices. They found Frank–van der Merwe layer-by-layer growth of mercury up to four layers on the ordered Cu surface.

In 1988, Onellion *et al.*[15] investigated mercury overlayers on silver. They reported that when mercury is melted at 160 K, where melting is defined as the temperature of initial mercury desorption from the surface, the mercury atoms ''wet'' the surface. In other words, the mercury atoms adjust themselves over the surface and move from their initial adsorption positions. The melting temperature for pure mercury at $1.013 \cdot 10^5$ Pa is 234.3 K.[16] Furthermore, Onellion *et al.*[15] suggested that clumping or island formation does not occur at the 1 to 2 ML coverage. They did not study the behavior of mercury at higher coverages, nor desorption of mercury beyond 160 K. However, Dowben *et al.*[12] say that islands form at mercury exposures of <10 L due to strong lateral interactions of the mercury.

Unertl and Blakely[17] found that Zn(0001) is completely covered by an oxide layer at a thickness of 2 to 3 MLs between 10^{-4} and 10^{-8} Pa, independent of temperature (between 77 and 425 K). However, the surface used in the aforementioned experiments was not specified. In 1996, Creemers[18] found that oxidized Zn(0001) forms a crystalline polar Zn terminated ZnO film. In other words, the oxygen atoms lie below the surface.

Furthermore, the adsorption of chlorine on Zn oxide has been studied by Grant *et al.*[19] They found a saturation of 0.30 chlorine adatoms per Zn site. They suggest that lateral interactions or kinetic effects prevent a higher rate of adsorption. It was previously reported by Hopkins and Taylor[20] that Cl_2 dissociates and adsorbs on ZnO(0001) at 300 K.

Chlorine contamination is known to originate in various sources in the environment. Some of these sources are due to saltwater, water purified with chlorine, and particulate salt in the atmosphere picked up from the ocean. This contamination can lead to chlorine deposition on metal surfaces exposed to the atmosphere. The present laboratory performed an earlier investigation on Zn and steel surfaces, which showed that chlorine naturally deposits on iron and Zn surfaces in quantifiable amounts.[21] Moreover, in 2003, Wang[22] stated that that the principal oxidized form of mercury in flue-gases from coal combustion is $HgCl_2$.

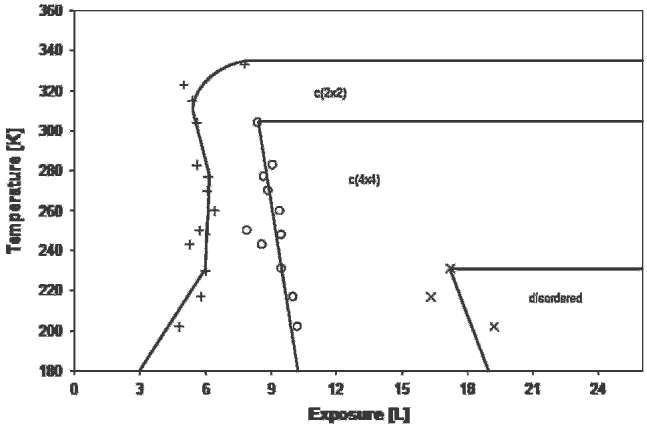

Fig. 1—Isobaric phase diagram showing adsorbed mercury structures on Cu(100).[12] A surface phase transition to a disordered phase occurs from mercury adsorption at higher exposures and decreased temperatures.

III. EXPERIMENTAL DETAILS

An ultra-high vacuum (UHV) chamber was used to conduct the TDAES experiments. A chlorine evaporator, Ar^+ ion sputter gun, and indirect sample cryogenator were mounted in the chamber. The sample temperature was reduced by liquid nitrogen. Desorption temperatures were monitored in the range of 82 to 298 K. Temperatures were kept constant during mercury dosing. A chromel/alumel thermocouple mounted on the manipulator adjacent to the sample holder was used to measure the sample temperature. Triply distilled mercury with a purity of 99.6 pct (supplied by Merck KGaA, Darmstadt, Germany) was dosed through a precision leak valve. The apparatus and experimental procedures have been reported previously.[9]

A precision leak valve was used to dose laboratory grade oxygen gas with a maximum of 1 ppm of impurities (supplied by Alfax, Kungsängen, Sweden), where gas dosing was controlled by a Langmuir dosage (one Langmuir is defined as $1.3 \cdot 10^{-4}$ Pa · s[13]). Chlorine was deposited onto the sample surface *via* an ionic cell. By applying a current to heat a silver chloride pellet, followed by applying a voltage, allows chlorine to recombine into Cl_2, which evaporated onto the sample surface. Exposures of chlorine were given in millicoulomb (mC), which related the ionic current to the application time.

The Zn sample was a pure crystal of (0001) orientation (supplied by Surface Preparation Laboratory (Zaandam, The Netherlands)). To compare effects of ordered and disordered surfaces, polycrystalline Zn was also selected for the study. This Zn was a 4-mm pellet (supplied by Merck (Darmstadt, Germany)) of 99.9 pct purity that was flattened and polished prior to cleaning. The Cu sample to be studied was polished oxygen-free high-purity Cu (supplied by Vacuum Generators (Hastings, United Kingdom)). The samples were cleaned before use by cyclic sputtering at RT. The base pressure in the chamber was less than $5 \cdot 10^{-8}$ Pa.

The experimental data were collected alternately over two kinetic energy intervals, namely, 30 to 230 eV and 20 to 1200 eV (where eV are electron volts, or the energy required to accelerate one electron through a potential difference of one volt[13]). This procedure was adopted to ensure good statistics of the intensity readings as well as to ensure that no contamination, interference of signals, or other problems affecting the experimental data occurred

during the experiment. The spectra were taken at approximately 6-minute intervals, and in all cases, the mercury, Zn, and Cu intensities measured from the two regions trended each other ideally. The Zn surface spectra were normalized to Zn at 994 eV using the respective elemental cross sections. The chlorine and oxygen signals have been amplified to demonstrate the features of the adsorption and desorption mechanisms. The LT polycrystalline Zn and the Cu spectra were normalized to mercury intensity. The combined error, primarily consisting of adjustment in sample position during heating and cooling of the manipulator inside the vacuum chamber, was estimated to be 15 pct of the intensity.

The TDAES spectra were recorded as derivative signals, $dN(E)/dE$, which were then translated into peak-to-peak heights. The detector efficiency was taken as proportional to the flux of detected electrons for the Auger transitions due to the constant peak width.[23]

IV. RESULTS

Mercury adsorption and desorption on Zn and Cu surfaces were studied at different doses, temperatures, and surface pretreatments, such as clean, oxidized, and chlorinated surfaces. These systems were examined for mercury saturation capacity at both RT (298 K) and LT (82 to 111 K). No mercury adsorbed at RT on either of the two Zn surfaces, but for the Cu surface, a ~0.27-nm-thick ML was formed. This value was calculated based on the classical mean free path for Cu.[13] The LT Cu system accepted more than one ML of mercury on the surface.

According to Paliwal *et al.*,[24] a mercury multilayer desorbs rapidly followed by slower desorption of the interface monolayer on the (111) face of silicon. This result is consistent with what has been observed for the systems in the present work.

A. *Zinc (0001)*

Dosing mercury at LTs onto Zn(0001) did not form a detectable layer on the surface, as presented in Figure 2. Although not presented here, the same result was observed for RT dosing of mercury on the Zn(0001) crystal.

The Zn(0001) crystal was pretreated separately with chlorine and oxygen, both at RT and LT, to compare their effects on mercury adsorption. Figure 3(a) shows the Zn crystal that was predosed with 0.42 mC chlorine at RT. Time was plotted against mercury exposure in the figure, where the chlorine and oxygen have been multiplied by a factor of 15 to amplify small concentration changes. The low energy Zn signal increases slightly, while the chlorine signal is reduced and finally removed completely. A comparison of this system was made at LT, as presented in Figure 3(b), where the same legend applies for both Figures 3(a) and (b). In this case, the surface was pre-exposed to 0.45 mC chlorine. Again, no mercury was detected at any dose. However, the effect of chlorine being stripped from the surface was more apparent. The chlorine coverage was also higher due to a higher sticking coefficient at LT.

The oxygenation of the Zn surface was carried out to 220 L prior to dosing mercury at 298 K to ensure surface saturation with oxygen,[25] as shown in Figures 3(c) and (d), where the same legend is applicable for both Figures 3(c) and (d). At RT, no mercury adsorbed onto the surface, as shown in Figure 3(c). At 111 K, mercury adsorbed in trace amounts, as shown in Figure 3(d). Although not presented here, experiments were conducted with a low dose of oxygen (~50 L) at both RT and LT. These experiments both resulted in zero mercury coverages.

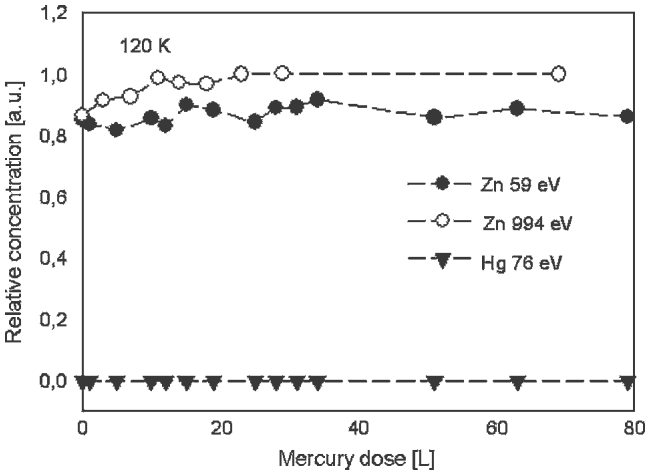

Fig. 2—No change in the relative surface concentration of Zn or mercury was observed during mercury dosing at 120 K on Zn(0001) using AES, indicating no mercury adsorption on the surface.

B. *Polycrystalline Zn*

Polycrystalline Zn naturally has more available sites for adsorption than a pure Zn crystal. This set of experiments on polycrystalline Zn showed very different results at LTs, but similar results of zero mercury coverage at RT, as compared to the pure crystal. Figure 4 depicts mercury dosed onto clean Zn at RT. There was no coverage of mercury.

Figure 5(a) presents adsorption of mercury onto polycrystalline Zn. In this case, mercury adsorbs. The T_1 and T_2 denote the initial desorption and the secondary desorption steps, respectively. The coverage was estimated to 0.31 nm at ~120 L mercury determined from the mean free path Zn Auger electrons. The thickness was calculated by the equation $I_s/I_o = e^{-x/\lambda}$ and the inelastic mean free path of Zn was taken to be 0.7 nm. The mercury intensity increased on annealing up to the initial desorption ~140 K; thereafter, desorption was rapid up to ~160 K, as seen in Figure 5(b). The increased intensity is not related to a higher coverage as the mercury pressure was turned off in the chamber, but is due to redistribution of mercury from islands to a smooth wetting layer prior to desorption, similar to mercury on Ag.[14] Roughly 1/3 ML of mercury remained at 236 K, which desorbed completely at RT. Here, ML coverage was determined by the saturation coverage at a constant temperature.

C. *Copper*

Copper has a high affinity for mercury.[26] The following figures present the mercury coverages obtained for various surface preparations on polycrystalline Cu and the temperatures at which desorption occurs.

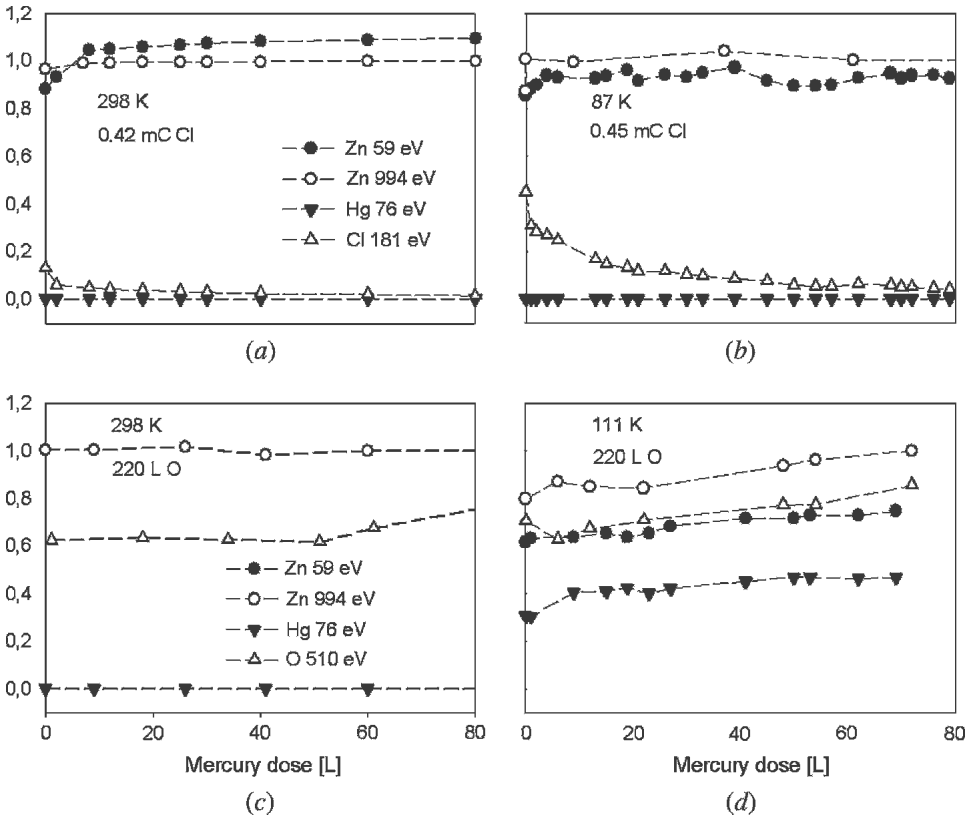

Fig. 3—Normalized relative surface concentrations plotted against mercury dose on Zn(0001) surface at constant pressure. The legend and scales are common for (*a*) and (*b*) and also for (*c*) and (*d*). (*a*) Dosing mercury on chlorinated Zn surface at 298 K removed surface chlorine. (*b*) Dosing of mercury on Zn surface chlorinated to 0.45 mC caused a sharper decrease in surface chlorine and no mercury adsorbed, where in (*a*) and (*b*) the chlorine has been amplified by 15 for clarity. (*c*) Dosing of mercury on oxygenated Zn surface at 298 K showed no reaction. (*d*) At 111 K, negligible changes in the surface were observed, within the error limits, where the oxygen signal was amplified by 15 in both (*c*) and (*d*).

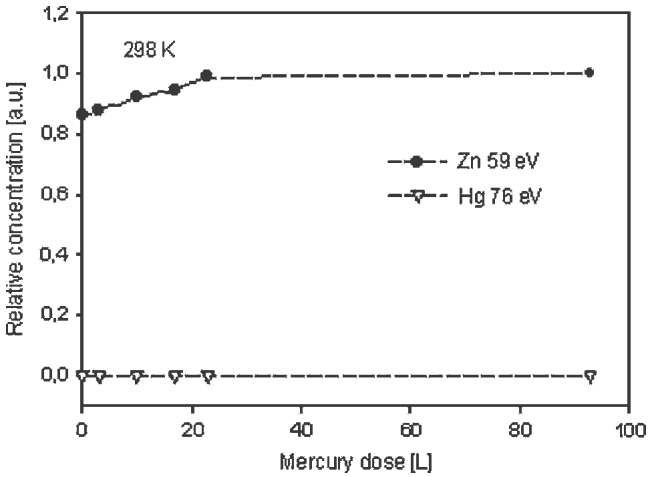

Fig. 4—Normalized relative concentration change plotted against mercury dose at RT. No mercury adsorbed to the Zn surface.

1. *Low temperature*

From Figure 6(a) at 68 L of dosed mercury, it is possible to see that the mercury coverage on the clean, polycrystalline Cu at the point, S_1, is 4.1 ML with a thickness of ~1.18 nm at 82 K, using the same calculations as with Zn, where the Cu signal has been amplified by a factor of 15 and the chlorine by 100. The thickness was calculated using the same intensity ratio equation as with Zn. The inelastic mean free path of Cu, λ_{Cu}, was taken to be 0.65 nm,[13] and the thickness, x, was calculated based on the difference in initial and saturation intensities. Desorption from this surface is shown in Figure 6(b). Desorption was rapid between 158 and 184 K, as denoted in Figure 6(b) by T_1 and T_2, respectively. Although not presented here, mercury did not fully desorb by RT. A second small desorption step occurred at 202 K, illustrated at point T_3 in Figure 6(b).

Compared to the clean Cu surface, the chlorinated Cu surface showed a higher mercury coverage of 1.35 nm at 87 K, shown by point S_2 in Figure 6(c). This corresponds to over 4.5 ML of mercury on the surface. Here, the Cu was chlorinated to 1.1 mC prior to dosing with mercury. Desorption began at nearly the same temperature as the clean Cu, at 162 K, as shown by T_1 in Figure 6(d). Desorption continued similarly to the clean Cu surface, but this time with a more pronounced step at around 200 K. The normalized chlorine points have been amplified by a factor of 100 to demonstrate the small increase and decrease corresponding to the surface mercury concentration.

Figure 6(e) presents mercury deposition on the oxidized Cu surface, where the oxygen signal has been amplified by 10 and the Cu signal by 10 to help illustrate the concentration changes. Oxygenation was carried out to 350 L prior to dosing with mercury. In this case, the mercury coverage reached ~0.74 nm, corresponding to just over 2.5 ML,

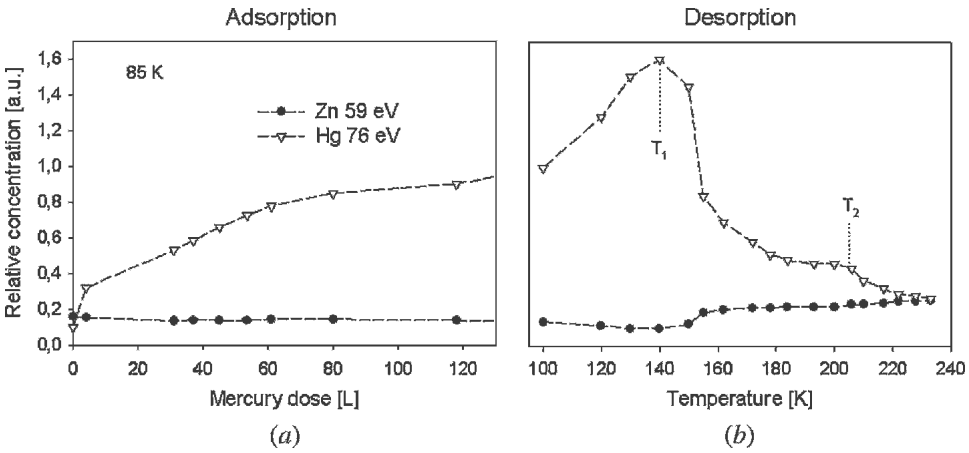

Fig. 5—The change in normalized relative surface concentration is plotted against mercury dose and then against the desorption temperatures: (*a*) multilayer mercury adsorption on polycrystalline Zn at 85 K; and (*b*) stepwise desorption of mercury from the surface, where T_1 and T_2 indicate desorption steps. The peak at 140 K prior to desorption is proposed to be due to a surface phase transformation of the mercury atoms.

shown by S_3 in Figure 6(e). Figure 6(f) shows desorption of mercury from the oxidized surface. Desorption was gradual, beginning at 150 K, as denoted by T_1 in Figure 6(f). Prior to desorption, the mercury signal increased at the same time as Cu was reduced, indicating a slight rearrangement of mercury wetting the surface similar to the polycrystalline Zn case at LT. Again, this may be due to a temperature-induced surface phase change. In a similar fashion as the clean and chlorinated Cu surfaces, a second desorption step was noted at 200 K, shown by T_2 in Figure 6(f). However, the oxidized surface began desorption at the lowest temperature.

In addition to dosing mercury on clean, chlorinated, and oxygenated Cu surfaces, it was of interest to study desorption of mercury from the Cu surface, initially dosed with mercury followed by dosing with chlorine or oxygen. These results are presented in Figure 7, where the Cu signal has been increased by a factor of 10 and the chlorine by 100 to amplify small changes. Copper was dosed with mercury to 60 L, and then dosed with chlorine to 0.25 mC, shown at point, P, in Figure 7(a). Naturally, the coverage of mercury is the same for both this system and for the clean Cu system, with just over 4 ML of mercury adsorbed. The chlorine affects desorption of mercury by decreasing the desorption temperature slightly. Desorption begins at 158 K on the clean surface, as compared to approximately 144 K on the postchlorinated Cu surface, due to $HgCl_2$ formation and desorption. The initial desorption temperature is shown at T_1 in Figure 7(b). At 184 K, desorption ceased, and at 202 K, a desorption step occurred, denoted by temperatures T_1 and T_2, respectively.

A Cu surface was dosed with mercury to 95 L then oxygen to study the interaction of the mercury and oxygen overlayers on the polycrystalline Cu. The dosing of oxygen on premercury-dosed Cu is presented in Figure 7(c). No change in the peak-to-peak heights of Cu or mercury, or any measurable signal from oxygen, was observed due to dosing with oxygen. Desorption, shown in Figure 7(d) at points T_1 and T_2 as the initial and final desorption layer temperatures, respectively, followed the desorption from the Cu-mercury system. However, a shift in the initial desorption temperature was observed.

2. *Room temperature*

Temperature is a critical parameter in mercury adsorption. Inasmuch, the RT coverage of mercury on polycrystalline Cu surfaces was examined. Figure 8(a) depicts clean Cu. Mercury reached nearly one ML of coverage (~0.27 nm). The Cu sample was also chlorinated to 1.4 mC, shown in Figure 8(b), where the chlorine signal was amplified by 50. In this case, mercury adsorbed similarly to the nonchlorinated surface. However, the chlorine signal was reduced during exposure similar to the Zn-chlorine-mercury case. Again, one may propose $HgCl_2$ formation and desorption.

Mercury adsorbed on oxidized Cu at RT to a similar level, shown in Figure 8(c), where the oxygen signal was enhanced by a factor of 10. Here, Cu was dosed to 18 L with oxygen. Copper had also been exposed to a high oxygen dose followed by dosing with mercury and showed a similar mercury coverage.

V. DISCUSSION

The adsorption of mercury on Zn and Cu systems has been studied. Factors involved in bonding and growth modes are discussed and compared. The Langmuir isotherm[27] has been used to calculate enthalpy data for specific systems and has been compared with literature values to support the arguments presented. Activation energies of desorption were also determined.

A. *Adsorption*

Surprisingly, mercury did not adsorb on Zn(0001) at LT or RT. Predosed chlorine was removed in mercury atmosphere, presumably due to $HgCl_2$ formation that desorbed immediately upon formation. Polycrystalline Zn displayed a higher capacity to adsorb mercury, where a coverage of 0.31 nm was reached at 85 K. However, at RT, no mercury was detected. In all cases, the dosing pressure was maintained at $1.3 \cdot 10^{-6}$ Pa.

The polycrystalline Cu behaved in a similar fashion: a higher mercury coverage was observed at LT than at RT. The LT chlorinated system adsorbed 4.7 ML of mercury,

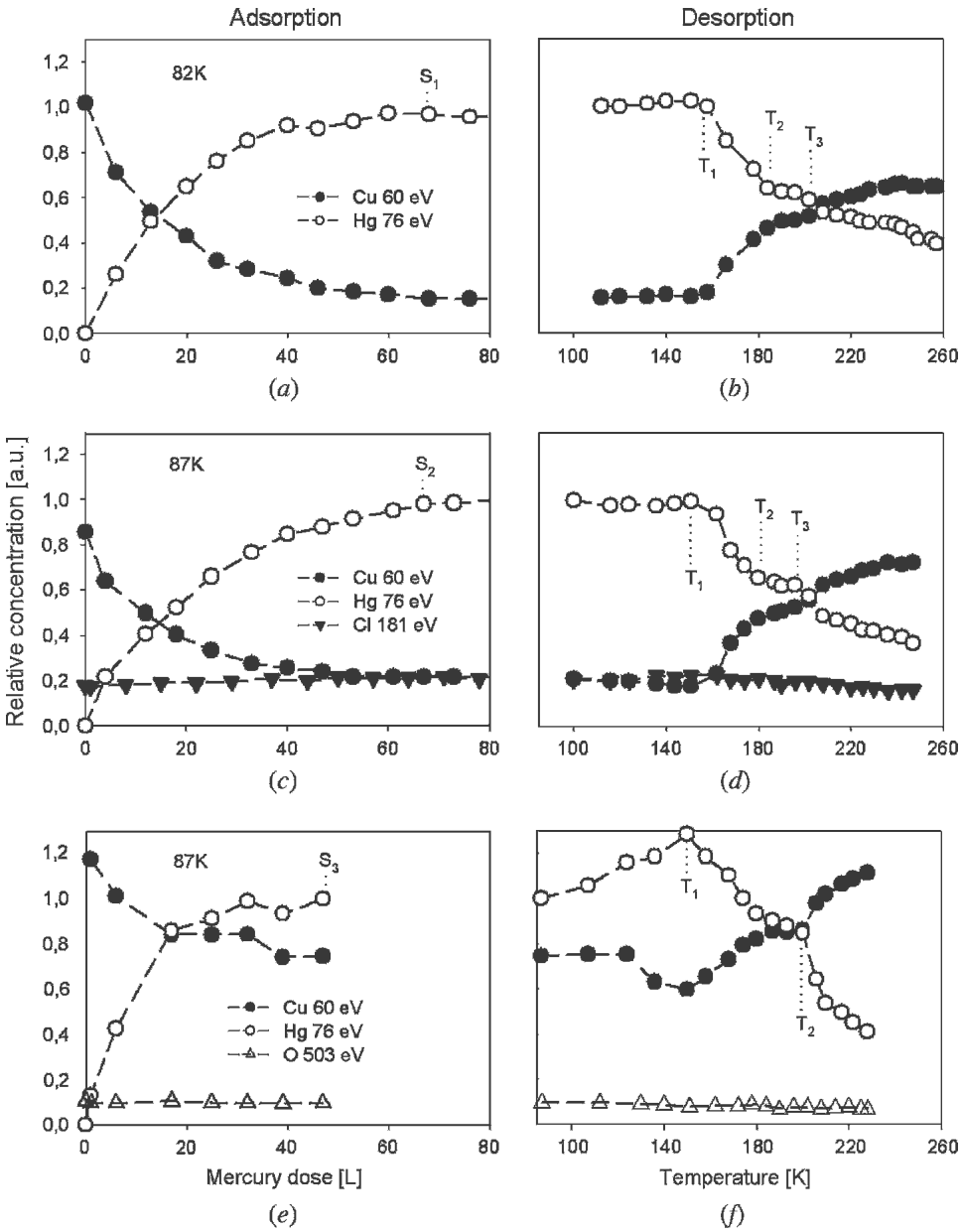

Fig. 6—Normalized relative surface concentrations plotted against mercury dose in the left column and desorption temperature in the right column. (*a*) Adsorption of mercury to saturation, S_1, at 4.4 ML on clean Cu at 82 K. (*b*) Rapid desorption of mercury from clean Cu between points T_1 and T_2, and T_3 indicates a second desorption step, where in (*a*) and (*b*) the Cu signal has been amplified by a factor of 15. (*c*) Adsorption of mercury to dosing saturation, S_2, at 5 ML on chlorinated Cu at 87 K. (*d*) Desorption of mercury from chlorinated Cu between T_1 and T_2, followed by a desorption step indicated by T_3, where for (*c*) and (*d*) the chlorine and Cu signals have been increased by a factor of 100 and 15, respectively. (*e*) Adsorption of mercury to less than 3 ML, S_3, on oxidized Cu at 87 K. (*f*) Stepwise desorption of mercury from oxygenated Cu, with desorption beginning at T_1 and with a desorption step at T_2, 200 K, where both the oxygen and Cu concentrations have been amplified by a factor of 10 for clarity.

which was thicker than the ~3 ML on the oxidized Cu at LT. The clean Cu system adsorbed nearly 4.1 ML of mercury at LT. The same trend was observed at RT, but with a lower coverage. The role of temperature is thus critical to mercury adsorption processes. In all cases, shown previously in Figures 5(a), 6(a), 6(c), 7(a), 7(c), and 7(e), mercury growth was laminar on the polycrystalline surface.

It appears that the first ML on Cu is chemisorbed and stable at RT, whereas following layers, adsorbed at LT, are weakly adsorbed on top of the first mercury ML. These layers desorb from the surface well before reaching RT.

The oxidation reduced bond strength of the first layer mercury, whereas desorption of additional layers occurred at the same temperatures as from the Cu surface. Chlorine appears to favor adsorption; however, these numbers are within the experimental certainty and should be interpreted with care. The slight increase may be due to a roughening reaction between chlorine and Cu that slightly increases the available surface area. Formation of $HgCl_2$ does not appear to be a plausible cause for a higher coverage because $HgCl_2$ is seen to desorb when the adsorption order is switched.

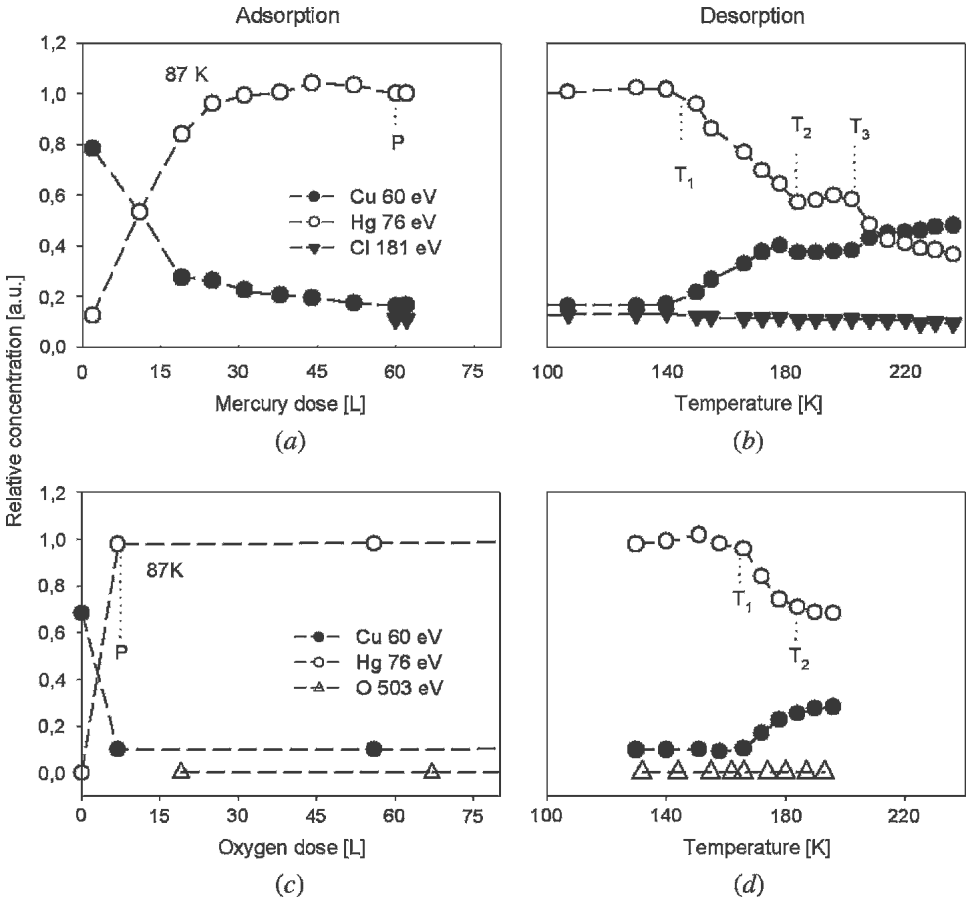

Fig. 7—(*a*) Mercury adsorption on Cu surface at 87 K, postchlorinated to 0.25 mC at point, P; and (*b*) followed by desorption. Temperatures T_1 and T_2 indicate the rapid desorption interval, followed by a desorption step beginning at T_3; (*c*) Cu surface predosed with 95 L mercury at point P at 87 K, followed by dosing with oxygen; and (*d*) desorption of the layer between temperatures T_1 and T_2. All Cu and chlorine concentrations have been amplified by a factor of 10 and 100, respectively.

Available literature values for the heats of formation, ΔH°_{298}, for the systems studied in this work are presented in Table I[28] On the basis of thermodynamics, it would be expected that the Zn-chlorine-mercury system would have the thickest mercury coverage for the Zn systems and similarly the Cu-chlorine-mercury system for the Cu systems. This was accurate for the Cu systems. On the Zn single crystal, the surface chlorine and oxygen coverages decreased according to the heats of formation. In other words, chlorine was removed much more than oxygen at LT, and at RT, only the chlorine reacted with the mercury and desorbed from the surface.

B. *Thermal Desorption*

A comparison of desorption temperatures for the Cu and Zn systems illustrates the dominant mechanisms involved in mercury desorption from the surfaces. For the clean and chlorinated Cu surfaces, desorption began at 158 and 162 K, respectively, followed by a second step at 202 K. From the preceding discussion, this can be assigned to desorption of different layers: first, the top most layers; then, at 202 K, the layer bonded to the interface mercury layer in contact with the substrate. As a consequence, the invariable desorption temperature is to be expected. Desorption of the interface layer can be expected to be influenced by the latter desorption, but this study is out of reach in the current study.

From the oxidized Cu surface, desorption began at 150 K and was not as rapid as in the previous cases. Initially, the surface Cu intensity decreased while the surface mercury intensity increased. From this, we conclude that the mercury bond to the oxidized surface is weakened compared to clean Cu. This affects the growth so islands are formed on oxidized Cu. This can be understood from the previously proposed strong intralayer mercury-mercury attraction.[12] Upon annealing, when the surface mercury melts, it wets the surface prior to desorption.

Desorption from polycrystalline Zn behaved similarly: the mercury concentration increased and the Zn concentration decreased before the concentrations reversed with increasing temperature. The initial desorption temperature was 140 K, where the surface phase transition occurred between ~100 and 140 K.

1. *Kinetics*

To quantitatively examine the bond strength of mercury, activation energies of desorption were calculated for both Zn and Cu systems. In the desorption regimes, time *vs*

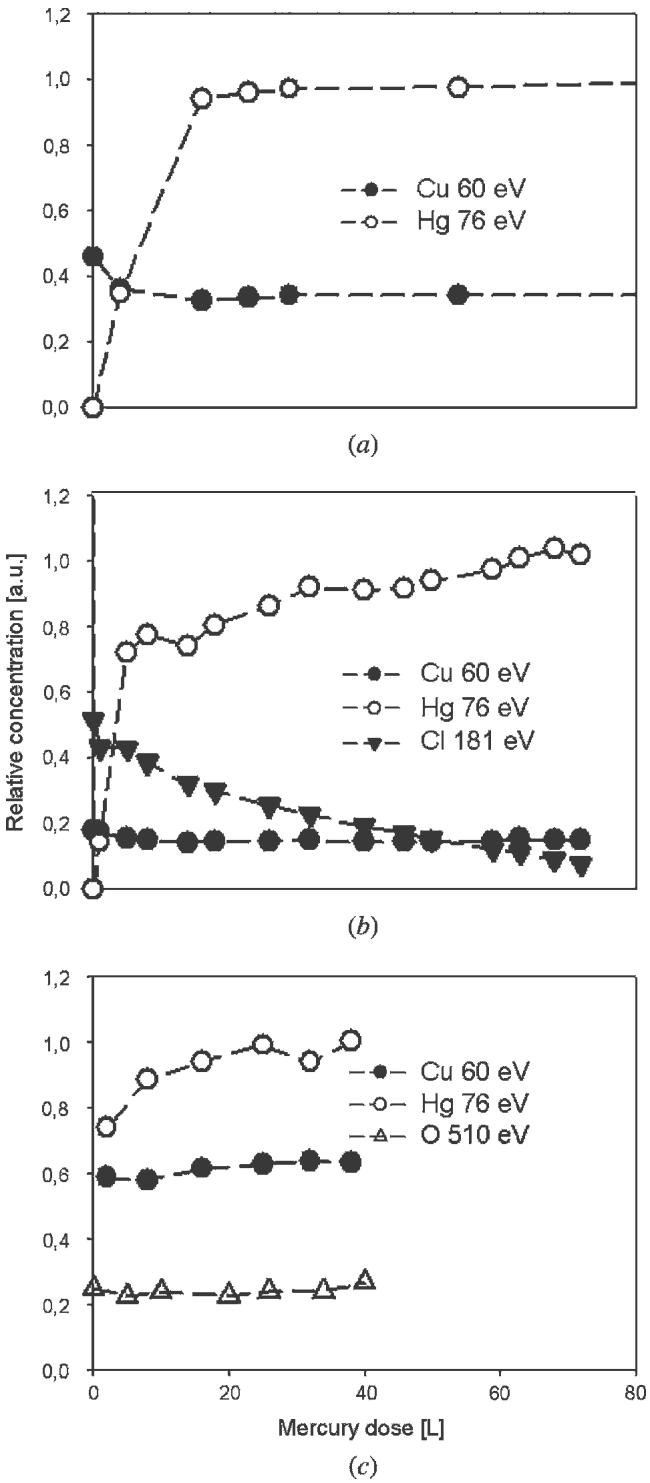

Fig. 8—(*a*) ML adsorption of mercury on clean Cu at 298 K; (*b*) adsorption of mercury at 298 K on Cu chlorinated to 1.4 mC, where chlorine has been increased by a factor of 50 for clarity; and (*c*) adsorption of mercury occurred on Cu oxidized to 18 L at 298 K, where the oxygen concentration has been amplified by a factor of 10 for clarity.

temperature relationships were derived and the heating rate was defined by

$$dT/dt = \beta \qquad [1]$$

To calculate the maximum peak temperature, T_P, the derivative of the intensity, dI_{Hg}/dT, was determined. The frequency factor, ν, was taken as 10^{13} Hz[11,23] according to literature values. For first-order desorption, the activation energy of desorption, E_d, is determined by the Redhead method[29] shown in Eq. [2].

$$E_d = \mathrm{R}T_P\left[\ln\left(\frac{\nu T_P}{\beta}\right) - 3.46\right] \qquad [2]$$

The results from these analyses are presented in Table II. These results are in the range of activation energy calculated by Jones and Perry[11] for mercury desorption from Fe(100) of 91 kJ mol^{-1} and for mercury desorption from the ordered Cu(100) crystal of 70 kJ/mol determined by Dowben *et al.*[12] At the lower system temperatures, mercury is desorbing from another mercury layer, and thus it makes sense that the desorption energies are lower than those determined by Dowben *et al.*[12]

2. *Desorption enthalpy*

The desorption reaction proceeds as follows:

$$Hg_{(s)} \leftrightarrow Hg_{(g)} \qquad [3]$$

The enthalpies were calculated based on the van't Hoff equation:

$$\frac{\partial \ln K_P}{\partial T} = \frac{\Delta H^o}{\mathrm{R}T^2} \qquad [4]$$

where K_P is the equilibrium constant and ΔH° is the standard enthalpy change. The fraction of occupied places on the surface (valid for each new layer) is set to

$$\theta_{Hg} = I/I_0 \qquad [5]$$

where I_0 denotes the pure intensity for a thick mercury multilayer at a constant pressure, P, of $1.3 \cdot 10^{-6}$ Pa. Assuming in the early desorption stages that the system behaves ideally such that θ_{Hg} approaches 1 as for a pure component, then the Langmuir Isotherm[27] can be used to solve for the equilibrium constant, K_P:

$$\theta(1 + K_P\,P) = K_P P \qquad [6]$$

Substituting K_P into Eq. [4] and plotting ln (K_P) against ($1/T$) yields the enthalpy value. The results are presented in Table III.

The Cu-oxygen-mercury system had the highest enthalpy value at 25.5 kJ/mol, with the Zn-mercury system having the next highest enthalpy value at 10.7 kJ/mol. This agrees well with the discussion regarding mercury wetting of the surface prior to desorption. The Cu-mercury and Cu-chlorine-mercury surface enthalpies were very similar, 8.3 and 7.9 kJ/mol, respectively, which agrees with the mercury coverage data.

C. *Practical Implications*

Due to natural and anthropogenic sources, mercury is known to have an atmospheric background level.[4,30] The rate of deposition of mercury from the atmosphere depends primarily upon the form of mercury in the vapor phase and

the proximity to emission sources. Elemental mercury is widely transported, up to several tens of thousands of kilometers, whereas oxidized or other mercuric species such as $HgCl_2$ are transported only up to several hundred kilometers from their source.[4,30] Species of particulate mercury are transported shorter distances.[4] It has also been suggested that due to temperature variations, mercury deposits in higher quantities in winter.[31]

In the present experimental study, it was shown that mercury deposition was greater at LTs than at RTs, and mercury adsorbs on both polycrystalline Zn and Cu. The chlorinated Cu surface had higher coverages than the clean Cu surface and much higher coverages than on the oxygenated Cu surface. At RT on polycrystalline Zn, no mercury adsorbed. However, at LT, mercury did adsorb.

Although no mercury adsorbed on the pure Zn crystal, the results were relevant. They showed that there is a reaction of mercury with chlorine but not with oxygen on Zn at RT. At LTs, mercury reacted more strongly with the chlorine and also with the oxygen. Mercury did not adsorb on Zn(0001), but chlorine and oxygen were stripped from it. From these results, it could be expected that galvanized scrap metal exposed to chlorine sources or stored near the coast will likely not trap mercury, but rather the mercury will react with the surface chlorine and decrease the scrap chlorine concentration. An oxidized surface would show the same effect, but because the reaction is weaker, it would not be noticeable except in controlled conditions.

When galvanized scrap metal is transported, it is often compacted and compressed against other steel surfaces. This friction may wear away the galvanized coating and expose the steel. From earlier work on iron surfaces,[9] it is known that mercury adsorbs one ML of mercury, to a thickness of 0.19 nm at 25 °C. Mercury adsorbed at LTs on clean iron remains on the surface at −20 °C and beyond 25 °C, albeit with a thickness of less than one ML of mercury. Therefore, mercury adsorbed on galvanized scrap may still have nearly 0.20 nm of mercury adsorbed on the clean surface.

Copper, as compared to Zn, is a virtual sink for mercury. Over one ML of mercury was formed on chlorinated Cu at RT. The oxidized surface even maintained some coverage of mercury at RT. Decreasing the temperatures to subzero conditions increased the mercury coverage by over 3 times on all of the Cu surfaces. At −20 °C, over one ML of mercury remained on the clean and chlorinated Cu surfaces. This corresponds to nearly 0.30 nm of mercury on the surfaces that remains at RTs. The oxygenated surface did not adsorb mercury at 25 °C, and less than 0.10 nm remained on the surface at −20 °C through 25 °C after adsorption of mercury at LTs. Therefore, natural surface oxides help to reduce mercury adsorption. Ensuring that Cu sources are not stored at LTs or by chlorine sources will help to reduce mercury adsorption on the surface.

Compared to the clean polycrystalline Zn surface, mercury adsorption is much greater at RTs and LTs on both the Cu and iron substrates.[9] Calculating for a 4 m^2 surface with 0.19 nm of mercury, assuming uniform and complete mercury saturation at −20 °C or RT, gives 10 mg of mercury. Similarly, 0.30 nm corresponds to 16 mg of mercury. This amount of mercury may become significant with extensive scrap iron stored outside LTs.

Further study is required for Zn to investigate the effects of chlorine and oxygen on nonmodel systems. It would also be useful to investigate the full effects of mercury trapped between surface layers that occur in practice, such as chlorine, sulfur, oxygen, or hydroxides. The extent of diffusion, if any, occurring in the surface and bulk layers would be of interest.

Table I. Literature Heat of Formation Values for Experimental Systems[28]

System	Component Basis	$-\Delta H^0_{298}$ (kJ/mol metal)	Error (kJ/mol)
Hg-O	Hg-O	90.8	0.8
Hg-Cl	$HgCl_2$	230.1	6.3
Zn-O	ZnO	348.1	1.3
Zn-Cl	$ZnCl_2$	416.3	1.3
Cu-O	CuO	155.2	3.3
Cu-CI	$CuCl_2$	205.9	10.5

Table II. Activation Energies of Desorption Using the Redhead Method[29]

Polycrystalline System	Maximum Peak Temperature, T_p(K)	Activation Energy, E_d(kJ/mol)
Zn-Hg	155	30
Zn-Hg	206	40
Cu-Hg	166	32
Cu-Hg	202	40
Cu-Cl-Hg	168	32
Cu-Cl-Hg	202	39
Cu-O-Hg	174	34
Cu-O-Hg	206	40

Table III. Enthalpy Values for Experimental Systems

System Name	Temperature Interval (K)	Desorption Enthalpy (kJ/mol)	Error (R^2)
Zn-Hg	[155, 233]	10.7	0.89
Cu-Hg	[112, 265]	8.3	0.83
Cu-Cl-Hg	[168, 247]	7.9	0.97
Cu-O-Hg	[174, 228]	25.5	0.94

VI. CONCLUSIONS

The aim of the current study has been to present and compare the effects of mercury dosing on a pure Zn crystal, pure polycrystalline Zn, and pure polycrystalline Cu substrates of various surface preparation conditions, in order to determine the source of mercury in scrap-based steelmaking. The Zn(0001) crystal showed no coverage of mercury at RT or LTs, regardless of the surface preparation. Polycrystalline Zn at LTs adsorbed a multilayer of mercury and proceeded to wet the surface prior to desorption, with less than 1 ML of mercury remaining on the surface at RT. Mercury reacted with predeposited chlorine and removed it from the Zn surface both at LTs and at RTs, due to $HgCl_2$ formation that bonded weakly with Zn.

Chlorinated polycrystalline Cu showed the highest mercury coverage of ~5 ML at LT. The clean Cu adsorbed just

over 4 ML of mercury, whereas the oxygenated Cu adsorbed closer to 2.5 ML of mercury at LT. Mercury formed less than 1 ML on clean Cu at RT, less than 1.5 ML on chlorinated Cu at RT and less than half of a ML on oxidized Cu at RT. Consequently, temperature plays an essential role in the adsorption of mercury on Zn and Cu.

The activation energies of desorption were calculated (Table II) and found to be in good accord with literature. Desorption temperatures were within 4 K of each other and the activation energies tracked each other closely. The oxygenated Cu had the highest activation energy of 34 kJ/mol, likely because of surface wetting. Clean polycrystalline Zn had the lowest activation energy, at 30 kJ/mol.

Based on these results, galvanized scrap cannot be considered a source of mercury in LT conditions. However, scrap containing Cu, such as electronic scrap, is prone to mercury adsorption and uptake.

ACKNOWLEDGMENTS

This study was gratefully supported by Jernkontoret and by a grant from the Department of Materials Science and Engineering at KTH. Special thanks are given to Associate Professor Birgitta Lindblad, M.Sc., for useful discussions and the Laboratory of Materials and Semiconductor Physics for generously providing the opportunity for scientific development in young students. Dr. Ragnhild E. Aune is also gratefully acknowledged for useful discussions and her support in this project. The experiments were financially supported by the Göran Gustafsson, the Carl Trygger, and the Wallenberg Foundations and the Swedish Research Council (VR).

REFERENCES

1. United Nations Environmental Programme: *Chemicals: Global Mercury Assessment*, Geneva, Switzerland, 2002, UNEP Chemicals, pp. 1-270.
2. J.L. Sznopek and T.G. Goonan: *US Geol. Survey Circ.*, 2000, No. 1197, pp. 1-32.
3. R.E. Aune and B. Lindblad: ISRN KTH/MSE–05/84–SE + THMETU/ART, Department of Metallurgy, KTH, Stockholm, 2001.
4. W. Schroeder and J. Munthe: *Atmos. Environ.*, 1998, vol. 32 (5), pp. 1-6.
5. M. Zettlitzer and W. Kleinitz: *Oil Gas-Eur. Mag.*, 1997, vol. 3, pp. 25-30.
6. S. Buchanan: *Met. Bull. Monthly*, 2004, vol. 401, pp. 42-43.
7. D. Lowrey: Master's Thesis, ISRN KTH/MSE–05/85–SE + THMETU/ART, Division of Metallurgy, KTH, Stockholm, 2001.
8. H. Okamoto: *J. Phase Equilib.*, 2002, vol. 23 (2), p. 196.
9. D. Roseborough, M. Göthelid, R.E. Aune, and S. Seetharaman: *Metall. Mater. Trans. B*, 2006, vol. 37, pp. 1049-56.
10. J. Wilcox and P. Blowers: *J. Mol. Struct.*, 2004, vol. 674, pp. 275-78.
11. R.G. Jones and D.L. Perry: *Vacuum*, 1981, vol. 31 (10–12), pp. 493-98.
12. P.A. Dowben, Y.J. Kime, C.W. Hutchings, W. Li, and G. Vidali: *Surf. Sci.*, 1990, vol. 230, pp. 113-22.
13. H. Lüth: *Solid Surfaces, Interfaces and Thin Films*, 4th ed., Springer, Berlin, 2001, pp. 34, 59, and 148.
14. W. Li, J.-S. Lin, M. Karimi, and G. Vidali: *J. Vac. Sci. Technol., A*, 1991, vol. 9 (3), pp. 1707-11.
15. M. Onellion, P.A. Dowben, and J.L. Erskine: *Phys. Lett. A*, 1988, vol. 130 (3), pp. 171-76.
16. *CRC Handbook of Chemistry and Physics 1999–2000: A Ready-Reference Book of Chemical and Physical Data*, 81st ed., D.R. Lide, ed., CRC Press, Boca Raton, FL, 2000.
17. W.N. Unertl and J.M. Blakely: *Surf. Sci.*, 1997, vol. 69, pp. 23-52.
18. C. Creemers: *Vacuum*, 1996, vol. 48 (6), pp. 553-59.
19. A. Grant, A. Jamieson, and C. Campbell: *Surf. Sci.*, 2000, vol. 458, pp. 71-9.
20. B.J. Hopkins and P.A. Taylor: *J. Phys. C: Solid State Phys*, 1976, vol. 9 (4), pp. 571-78.
21. D. Roseborough: unpublished research, ISRN KTH/MSE–05/91–SE + THMETU/ART, Department of Materials Process Science, KTH, Stockholm, 2003.
22. J. Wang, B. Clements, and K. Zanganeh: *Fuel*, 2003, vol. 82, pp. 1009-11.
23. S.J. Pratt, D.K. Escott, and D.A. King: *Phys. Rev. B*, 2003, vol. 68, pp. 235406-1-235406-11.
24. V. Paliwal, A.G. Vedeshwar, and S.M. Shivaprasad: *Phys. Rev. B*, 2002, vol. 66, pp. 245404-1-245404-5.
25. J. Weissenrieder, M. Göthelid, M. Månsson, H. von Schenck, O. Tjernberg, and U.O. Karlsson: *Surf. Sci.*, 2003, vol. 527, pp. 163-72.
26. *Binary Alloy Phase Diagrams*, T.B. Massalski, J. Murray, L.H. Bennett, and H. Baker, eds., ASM, Metals Park, 1987, vol. 1, p. 1069.
27. J. Szekely, J.W. Ewans, and H.Y. Sohn: *Gas-Solid Reactions*, Academic Press, New York, NY, 1976.
28. O. Kubaschewski, E.L.L. Evans, and C.B. Alcock: *Metallurgical Thermochemistry,* 4th ed., Pergamon Press, Oxford, United Kingdom, 1967, pp. 372-88.
29. J.W. Niemantsverdriet: *Spectroscopy in Catalysis—An Introduction*, VCH, Weinheim, 1993, pp. 28-32.
30. L. Poissant, M. Pilote, X. Xiaohong, Z. Hong, and C. Beauvais: *J. Geophys. Res.*, 2004, vol. 109 (D11), pp. D11301-11.
31. Å. Iverfeldt: *Water, Air, Soil Pollut.*, 1991, vol. 56, pp. 251-65.